Free Expansion of a Pure Electron Plasma Column

J. D. Moody[a] and J. H. Malmberg
Physics Department, University of California, San Diego, La Jolla, California 92093
(Received 12 March 1992)

The collective free expansion of a magnetized pure electron plasma column along the confining axial magnetic field is experimentally and theoretically investigated. A new hydrodynamic theory for nonlinear plasma wave evolution in a bounded cylinder is described which predicts the experimental results. The plasma free expansion is initially characterized by a self-similar plasma flow resulting in a perturbed density and velocity with no characteristic length scale.

PACS numbers: 52.35.Mw, 52.25.Fi, 52.25.Wz, 52.35.Fp

Large-amplitude (nonlinear) electron plasma wave disturbances in a magnetized plasma column represent a broad area of interesting plasma physics phenomena. Three types of nonlinear disturbances which have been studied in detail in neutral plasmas are (1) electron plasma solitons [1-3], (2) electron holes [3-6], and (3) electron plasma shock waves [7]. We have experimentally investigated another type of large amplitude electron plasma wave phenomenon which has received a considerable amount of theoretical attention in neutral plasmas [8-11] but little experimental study in either neutral or nonneutral plasmas [12]. This phenomenon, which is characteristically different from the three phenomena just listed, is the free expansion of a pure electron plasma column along the axial confining magnetic field.

Measurements of the radially averaged density made at several positions along the plasma column indicate that during plasma free expansion, a rarefaction disturbance propagates into the plasma at a speed which is within $\pm 10\%$ of the phase speed of long-wavelength electron plasma waves. The average plasma density behind the disturbance decreases to $\sim \frac{1}{2}$ of the initial average density. When the disturbance reaches the other end of the plasma column it is reflected, causing the remaining plasma density to decrease, eventually emptying the confinement region of plasma.

Figure 1 shows a schematic view of the experimental apparatus used in this study. The pure electron plasma column is contained radially by a uniform axial magnetic field and axially by electrostatic potentials applied to segments of a conducting cylinder surrounding the plasma. The properties of a pure electron plasma confined in this type of device have been extensively investigated [13]. The conducting cylinder diameter is 6.1 cm. The plasma radial density profile is typically bell shaped with a FWHM of about 3 cm. The axial confinement potentials range between -50 and -150 V and the plasma column is either 113 or 100 cm long, contained between rings G1 and S2 or G4. The experiments were conducted with the following plasma parameters: axial magnetic field $280 \leq B \leq 630$ G; central plasma density 3×10^6 cm$^{-3} \leq n_0 \leq 8\times10^6$ cm^{-3}; space charge potential on axis [14] of about -12 V for $n_0 = 7\times10^6$ cm^{-3}; parallel electron temperature 1 eV $\leq T_\parallel \leq 18$ eV; electron collision frequency 6 sec$^{-1} \leq \nu_{ee} \leq 7\times10^2$ s^{-1}, and background neutral pressure of $\sim 5\times10^{-10}$ Torr. While the axial confining potentials and magnetic field are applied, the background transport of the plasma causes the central density to decrease to $\frac{1}{2}$ of its initial value in about 200 ms.

The plasma typically undergoes a three-stage life cycle consisting of injection, hold, and dump. The cycle-to-cycle variation in plasma parameters is about 0.1%. The plasma temperature at the beginning of the hold cycle is 1 eV $\pm$ 0.2 eV. Compressional heating is sometimes used to increase the temperature up to a maximum of 18 eV $\pm$ 2 eV. This is done by applying a 10-kHz square-wave voltage, which oscillates between ground and -40 V, to either ring L1 or L4. The signal is applied for up to 40 ms depending on the desired final temperature. The temperature is determined by measuring the charge which escapes from the confinement region when the confinement potential is switched to an intermediate value between ground and the initial confinement potential [15].

Time-dependent changes in the radial average plasma density at a particular axial location are measured by monitoring the image charge on the ring at the corresponding axial position. A cable with stray capacitance of about 1×10^{-10} F connects the ring to the input of a

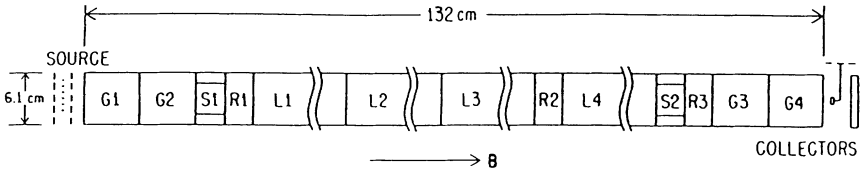

FIG. 1. Schematic view showing the conducting ring structure of the experimental apparatus.

low-noise, 30-dB inverting amplifier with a 5-MHz bandwidth. The amplifier input capacitance is about 2.3×10^{-10} F and the input is grounded through a 20-MΩ resistor. The ring capacitance is negligible. Plasma injection produces a negative radial electric field at the surface of the ring. This field causes positive image charge to be drawn off of the amplifier input and the connecting cable and accumulate almost instantly on the ring. A voltage (typically -10 to -20 mV) appears on the ring, cable, and amplifier input which exponentially decays to 0 V with an RC time constant of about 6 ms. The image charge Q_0 on the ring is equal and opposite to the total charge contained in a length of plasma equal to the length of the ring.

The free expansion is initiated by grounding the confinement ring at the collector plate end. A mechanical relay is used to achieve a switching time of approximately 25 ns. The collector plate is biased at a constant +90 V in order to reduce the effect of secondary electron emission from the plate. As the plasma expands out of the confinement region the negative radial electric field at the ring surfaces decreases in magnitude. This causes positive image charge to leave the ring and accumulate almost instantly on the cable and amplifier input. A positive voltage develops on the ring, cable, and amplifier which decays with about a 6-ms time constant. This voltage is closely proportional to $Q(t) - Q_0$ for the entire duration of the free expansion (< 40 to 50 μs) since there is negligible voltage decay during this time. The quantity $Q(t)$ represents the total charge at time t contained in a length of plasma equal to the ring length. The voltage at the amplifier input is inverted and amplified. The output is then normalized to $|Q_0|$ and offset by unity giving a signal equal to $Q(t)/Q_0$. The traces displayed in Fig. 2 are plots of $Q(t)/Q_0$ versus time t.

Figure 2(a) shows that when ring G4 is grounded, the signal on S2 remains unchanged for a short time while the rarefaction front propagates from ring G4 to S2. The signal then drops quickly and approaches a plateau value. After some additional time delay the signal on R2 begins to drop and approaches the same plateau level. There is a longer time delay of about 780 ns before the signal on ring R1 begins to drop. The propagation speed of the front is calculated from this 780-ns delay time and the distance between rings to be 1.3×10^8 cm/s. Separate measurements using various electrodes indicate that the front propagates at a constant speed through the plasma column. The R2 and S2 signals continue to approach the plateau value until the rarefaction front returns from reflection off of the confined end of the plasma column. At this time, the R2 and S2 signals drop below the plateau value with R2 dropping slightly earlier than S2. The three signals then merge as they asymptotically approach zero. The R1 signal at the far end of the column never exhibits a plateau but drops steadily.

Figure 2(b) shows measurements from a shorter plasma column. A shorter column allows a measurement to

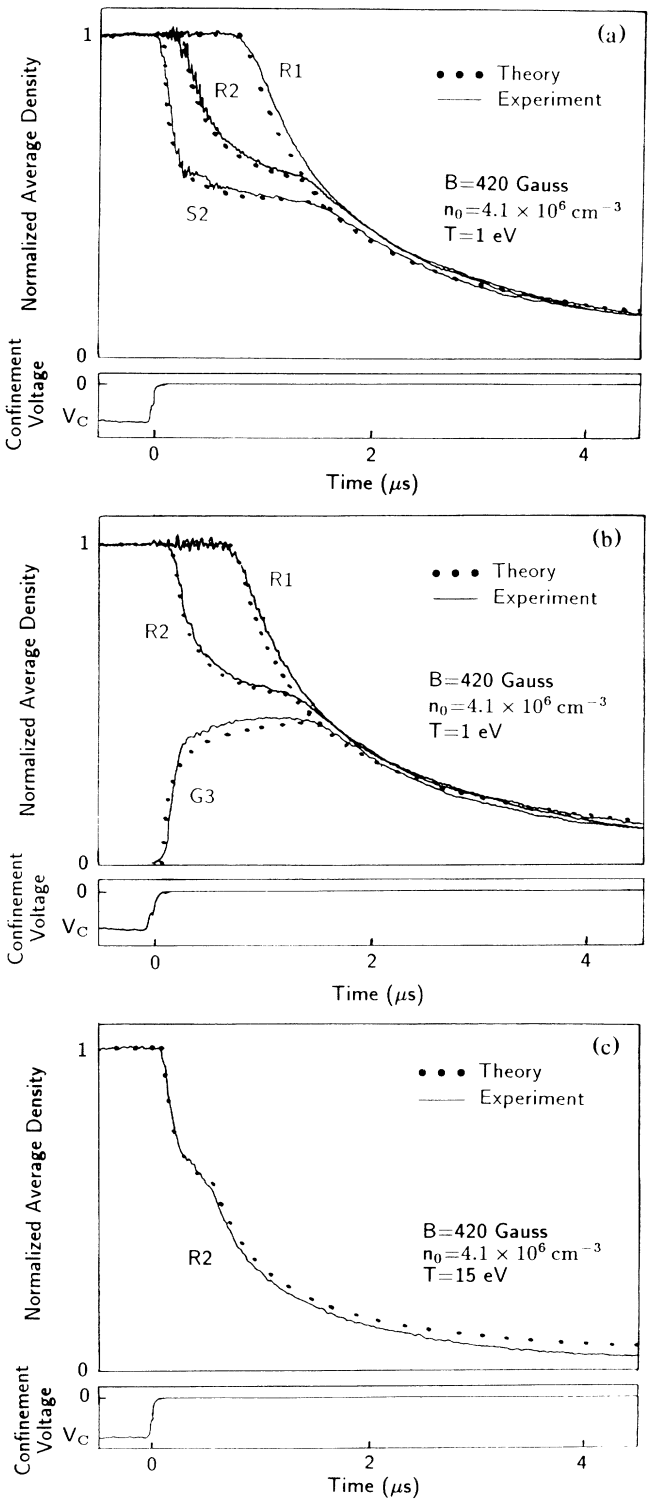

FIG. 2. Experimental and theoretical ring signals as a function of time for a typical plasma free expansion. Also shown is the confinement potential on ring G4, S2, or G3. (a) The plasma column is 113 cm long (confining potentials applied to G1 and G4). (b) The plasma column is 100 cm long (confining potentials applied to G1 and S2). (c) The plasma column is 100 cm long (confining potentials applied to G2 and G3) and $T = 15$ eV ($\lambda_D/a \sim 0.95$).

be made at ring G3 where initially there is no confined plasma. The R1 and R2 signals for this case are similar to the longer column case. The G3 signal is initially zero but begins to rise approximately 50 ns after ring S2 is grounded. Both G3 and R2 then approach the same plateau value. The return of the reflected rarefaction front is marked by G3 and R2 falling away from the plateau value. All three signals then merge as they approach their asymptotic value indicating zero remaining plasma density.

We have measured the speed of the rarefaction front for central plasma densities ranging from 4×10^6 cm^{-3} to 8×10^6 cm^{-3}, magnetic fields ranging from 280 to 560 G, and temperatures ranging from 1 to 18 eV. The speed (which ranges between 1 and 5 times the thermal speed) is always within 10% of the measured phase speed of a small amplitude long wavelength electron plasma wave in the same plasma column. We have numerically calculated the dispersion relation of linear standing waves in the pure electron plasma column [16] and the results agree with the measured dispersion. As expected from the results of Trivelpiece and Gould [17] the dispersion relation is acousticlike for long wavelength modes.

The basic physics of the free expansion process is that the electrons escape from the confinement region as a result of (1) electrostatic pressure and (2) ballistic free streaming. The effect of electrostatic pressure dominates the dynamics for plasma temperatures less than about 15 eV, where $\lambda_D/a<1$ (λ_D is the plasma Debye length and a is the plasma radius), and this suggests a hydrodynamic description. We have developed a hydrodynamic theory which contains this basic physics and which predicts the experimental results at low to moderate plasma temperatures. Previously, Manheimer has described one hydrodynamic model for the nonlinear steepening of an electron plasma wave in a bounded cylindrical cold plasma [18]. His theory retains only the lowest-order linear radial mode for describing the nonlinear radial evolution. In contrast, the theory described here determines the exact radial evolution during free expansion of a bounded cylindrical warm plasma. Finite temperature is included by a scalar pressure term in the momentum conservation equation and an adiabatic equation of state.

The plasma dynamics are described by the four hydrodynamic equations:

$$\frac{\partial n}{\partial t}=-\frac{\partial}{\partial z}(nv)\,, \tag{1}$$

$$\frac{\partial v}{\partial t}=-v\frac{\partial v}{\partial z}+\frac{e}{m}\frac{\partial\phi}{\partial z}-\frac{1}{mn}\frac{\partial P}{\partial z}\,, \tag{2}$$

$$\nabla_\perp^2\phi\simeq\nabla^2\phi=4\pi en\,, \tag{3}$$

$$\frac{d}{dt}\left(\frac{P}{n^\gamma}\right)=0\,, \tag{4}$$

where ϕ, v, n, and P are the plasma potential, axial directed local fluid velocity, density, and pressure; γ is the ratio of specific heats, m is the electron mass, and e is the magnitude of the electron charge. The large magnetic field confines the particle dynamics to be one dimensional so that the ratio of specific heats, γ, is taken to be 3. The two S rings in Fig. 1 are divided into four equal azimuthal sectors. Separate measurements from each sector on both rings indicate that the plasma free expansion is cylindrically symmetric. As a result we assume cylindrical symmetry in the theory. The initial temperature (prior to free expansion) is known to be about 30% higher at the plasma edge than at the plasma center. This temperature variation is assumed to have only a minor effect on the theoretical predictions so that a constant initial temperature is assumed in the theory. The axial density variation of the rarefaction disturbance in a length of one plasma radius is typically small. This allows $\nabla^2\phi$ in the Poisson equation to be replaced with $\nabla_\perp^2\phi$. Equation (4) indicates that the plasma flows along each field line at constant entropy. This allows us to write the last term in Eq. (2) as $-(3\kappa T/m)(1/n)\partial n/\partial z$ where the local temperature and density during free expansion are related as $T=T_0(n/n_0)^2$.

We use the fluid model to describe the free expansion of a plasma column confined between $z=0$ and $z=-L$. The plasma density is assumed to be constant along each field line and to fall abruptly to zero at either end of the column. The plasma is assumed to have zero initial fluid velocity. At $t=0$ the confinement is instantaneously removed from $z=0$ allowing the plasma to freely expand. These initial and boundary conditions possess no scale length so that the solution to Eqs. (1)–(4) is of the self-similar type [19] with z and t appearing only as the ratio z/t.

The self-similar solution to Eqs. (1)–(4) is obtained by converting the partial differential equations to ordinary differential equations with the independent variable $\zeta\equiv z/t$. The density and pressure are written as $n(r,z,t)=\xi(r)\bar{n}(r,z,t)$ and $P(r,z,t)=\xi(r)\bar{P}(r,z,t)$ [where $\bar{n}(r,z,t)=n_0+\delta n(r,z,t)$ and $\bar{P}(r,z,t)=P_0+\delta P(r,z,t)$ and $\xi(r)$ gives the equilibrium density radial dependence]. The continuity equation (1) can be integrated to give $\bar{n}/n_0=c_0/(v-\zeta)$, where c_0 is the rarefaction front speed. Using Eqs. (2), (4), and the expression for $\bar{n}/n_0$, the ζ derivative of the Poisson equation (3) is written as

$$\frac{1}{r}\frac{d}{dr}r\frac{d}{dr}\left(\frac{d\phi}{d\zeta}\right)+\frac{\bar{\omega}_p^2}{V^2}\xi(r)\frac{d\phi}{d\zeta}=0 \tag{5}$$

and the momentum conservation equation is written as $d\bar{n}/d\phi=-(e/m)(\bar{n}/V^2)$, where $\bar{\omega}_p^2=4\pi\bar{n}e^2/m$ and $V^2=(c_0n_0/\bar{n})^2-(3\kappa T_0/m)(\bar{n}/n_0)^2$. The solution to Eq. (5) with zero radial nodes is chosen to construct the self-similar solution so as to agree with the measured front propagation speed. The numerical solution to Eq. (5) gives $\bar{n}$, v, and ϕ as functions of ζ. The actual solution for $\bar{n}$, v, and ϕ at any value of z and t can then be determined from these three functions.

The plasma flow velocity at $z = -L$ is set to zero causing a reflection to occur when the rarefaction front reaches this point. The evolution of the density and velocity in the region between $z = -L$ and the reflected front is no longer self-similar but can be determined from Eqs. (1)–(4) by using the method of characteristics [20–22].

The radially averaged density predicted by the new hydrodynamic theory is compared with the measurements in Fig. 2. The theory closely predicts (1) the initial time at which the signals on R1, R2, S2, and G3 begin to change, (2) the approach of the signals toward a plateau, (3) the duration of this plateau before the reflected front returns to the location of each ring, and (4) the long-time behavior of the signals. Agreement between the fluid model and the measurement at higher temperature where ballistic effects begin to become important is also good, as is shown in Fig. 2(c). This suggests that the new fluid model works well in the warm as well as the cold plasma regimes. A plot of the data in Fig. 2(a) with $\zeta = z/t$ as the x axis would show the signals from R2 and S2 to lie on top of each other for $t \lesssim 1.4$ μs, confirming that the free expansion is self-similar during this time.

We have made a number of measurements to determine the sensitivity of our results to the assumptions in the theory. For example, we have varied the end shape of the plasma column by varying the confinement potential from -30 to -180 V and found only a few percent variation in the measured signals. In addition, we have varied the voltage switching time on the confining ring (ring G4 or S2 in Fig. 1) from about 10 to 100 ns and found that the measured signals experienced only a shift in time. We have also produced a slightly non-Maxwellian initial distribution function by plasma wave heating and found that this resulted in only a few percent change in the measured signals. We have additionally checked one interesting result from the hydrodynamic theory which is that a small amplitude plasma wave excited in the region $z > 0$ cannot propagate into the region $z < 0$ for times during which the self-similar solution is valid at $z \sim 0$. Using the same experimental arrangement as used for the results shown in Fig. 2(b) we have applied varying amplitude positive voltage pulses to rings R3 and G3 during plasma free expansion and have observed no measurable response on rings L4, R2, and L3.

In summary, we have described a new hydrodynamic theory for nonlinear plasma wave evolution in a bounded cylinder which shows good agreement with the free expansion measurements. We believe that for low to moderate plasma temperatures the basic physics of the free expansion process is contained in this new theory.

J.D.M. acknowledges useful insights from Dr. F. J. Moody. In addition, helpful discussions with Dr. T. M. O'Neil, Dr. D. Dubin, and Dr. R. A. Smith are gratefully acknowledged. This work was supported by U.S. Department of Energy Grant No. DE-FG03-85ER53199 and NSF Grant No. NSFPHY87-06358.

[a]Present address: Lawrence Livermore National Laboratory, P.O. Box 5508, Livermore, CA 94550.

[1] H. Ikezi, P. J. Barrett, R. B. White, and A. Y. Wong, Phys. Fluids **14**, 1997 (1971).

[2] V. I. Karpman, J. P. Lynov, P. Michelsen, H. L. Pécseli, J. Juul Rasmussen, and V. A. Turikov, Phys. Rev. Lett. **43**, 210 (1979); Phys. Fluids **23**, 1782 (1980).

[3] J. P. Lynov, P. Michelsen, H. L. Pécseli, J. Juul Rasmussen, K. Saeki, and V. A. Turikov, Phys. Scr. **20**, 328 (1979).

[4] K. Saeki, P. Michelsen, H. L. Pécseli, and J. Juul Rasmussen, Phys. Rev. Lett. **42**, 501 (1979).

[5] H. Schamel, Phys. Scr. **20**, 336 (1979).

[6] M. Kako, T. Taniuti, and T. Watanabe, J. Phys. Soc. Jpn. **31**, 1820 (1971).

[7] K. Saeki and H. Ikezi, Phys. Rev. Lett. **29**, 253 (1972); K. Saeki, J. Phys. Soc. Jpn. **35**, 251 (1973).

[8] Ch. Sack and H. Schamel, Phys. Fluids **29**, 1337 (1986), and references therein.

[9] J. E. Allen and L. M. Wickens, J. Phys. **40**, C7-547 (1979).

[10] A. V Gurevich, L. V. Pariĭskaya, and L. P. Pitaevskiĭ, Zh. Eksp. Teor. Fiz. **49**, 647 (1965) [Sov. Phys. JETP **22**, 449 (1966)].

[11] J. E. Crow, P. L. Auer, and J. E. Allen, J. Plasma Phys. **14**, 65 (1975).

[12] Y. C. Saxena and P. I. John, in *Proceedings of the International Conference on Plasma Physics, Nagoya, Japan, 7–11 April 1980,* edited by K. Takayama (Fusion Research Association Japan, Nagoya, 1980), Vol. 1, p. 125.

[13] *Non-Neutral Plasma Physics,* edited by C. W. Roberson and C. F. Driscoll, AIP Conf. Proc. No. 175 (AIP, New York, 1988), pp. 1–74.

[14] We calculate the space charge potential from the line-integrated density as a function of radius which is measured using the radially moveable collector shown just to the right of ring G4 in Fig. 1.

[15] D. L. Eggleston, C. F. Driscoll, B. R. Beck, A. W. Hyatt, and J. H. Malmberg, Phys. Fluids B **4**, 3432 (1992).

[16] J. H. Malmberg and J. S. deGrassie, Phys. Rev. Lett. **35**, 577 (1975).

[17] A. W. Trivelpiece and R. W. Gould, J. Appl. Phys. **30**, 1784 (1959).

[18] Wallace M. Manheimer, Phys. Fluids **12**, 2426 (1969).

[19] L. D. Landau and E. M. Lifshitz, *Fluid Mechanics* (Pergamon, New York, 1987), 2nd ed., p. 366.

[20] A. H. Shapiro, *The Dynamics and Thermodynamics of Compressible Fluid Flow* (The Ronald Press Company, New York, 1953), pp. 128–131 and 462–528.

[21] F. J. Moody, *Introduction to Unsteady Thermofluid Mechanics* (Wiley, New York, 1990), pp. 253–285 and 444–454.

[22] J. D. Moody and J. H. Malmberg (to be published).